

# All electrical measurement of the density of states in (Ga,Mn)As

D. Neumaier,<sup>\*</sup> M. Turek,<sup>†</sup> U. Wurstbauer,<sup>‡</sup> A. Vogl, M. Utz, W. Wegscheider, and D. Weiss  
*Institut für Experimentelle und Angewandte Physik,*  
*University of Regensburg, 93040 Regensburg, Germany*  
 (Dated: November 10, 2018)

We report on electrical measurements of the effective density of states in the ferromagnetic semiconductor material (Ga,Mn)As. By analyzing the conductivity correction due to enhanced electron-electron interaction the electrical diffusion constant was extracted for (Ga,Mn)As samples of different dimensionality. Using the Einstein relation allows to deduce the effective density of states of (Ga,Mn)As at the Fermi energy.

PACS numbers: 71.20.-b, 75.50.Pp, 73.23.-b

The ferromagnetic semiconductor (Ga,Mn)As [1] has been studied intensely over the last decade and has become a model system for future spintronics applications [2, 3]. With typical Mn-concentrations between 1 % and 15 % maximum Curie temperatures of up to  $\sim 180$  K have been reported [4, 5]. Mn atoms on Ga-sites provide both holes and magnetic moments. For Mn concentrations larger than 1 % the impurity wavefunctions at the Fermi energy overlap and a metallic state forms. The ferromagnetic order between the magnetic moments of the Mn-ions is mediated by the delocalized holes [6]. A topic of current debate is whether the holes reside in an impurity band, detached and above the valence band or in the valence band [7]. A mean field picture based on the latter scenario allowed to predict, e.g. Curie temperature [6] or magnetocrystalline anisotropies [8] in (Ga,Mn)As correctly. On the other hand optical absorption experiments, carried out, e.g. in Ref. [9, 10], suggest that even for high manganese concentrations of up to 7 % the Fermi energy stays in an impurity band, detached from the valence band, with a high effective hole mass of order ten free electron masses  $m_e$  [9]. However, there is also indication that the impurity band and the valence band have completely merged as discussed in Ref. [7] and references therein. In the present letter we make use of the well known quantum mechanical conductivity correction due to electron-electron interaction (EEI) to extract the diffusion constant and hence the density of states at the Fermi energy,  $N(E_F)$ . The electrically measured values of  $N(E_F)$  will be compared with recent theoretical calculations.

In ferromagnetic (Ga,Mn)As the conductivity is decreasing with decreasing temperature below 10 K. This conductivity decrease can be explained by enhanced electron-electron interaction [11]. The effect of EEI arises from a modified screening of the Coulomb-potential due to the carriers' diffusive motion and depends on the dimensionality of the conductor [12]. As the conductivity decrease due to enhanced electron-electron interaction is depending on the electrical diffusion constant  $D$ , a detailed analysis of the conductivity decrease, different for different dimensionality, provides experimental access

Sample	$l$ ( $\mu\text{m}$ )	$w$ ( $\mu\text{m}$ )	$t$ (nm)	$N$	$T_C$ (K)	$p$ ( $10^{26} / \text{m}^3$ )
$1_{1D}$	7.5	0.042	42	25	90	3.8
$1_{1DA}$	7.5	0.042	42	25	150	9.3
$2_{1D}$	7.5	0.035	42	12	90	3.8
$1_{1D-2DA}$	10	0.067	30	25	150	8.6
$2_{1D-2DA}$	10	0.092	30	25	150	8.6
$3_{1D-2DA}$	10	0.170	30	25	150	8.6
$4_{1D-2DA}$	10	0.242	30	25	150	8.6
$1_{2D}$	180	11	42	1	90	3.8
$1_{3D}$	240	10	150	1	?	1.4
$2_{3D}$	240	10	300	1	75	2.1

TABLE I: Length  $l$ , width  $w$ , thickness  $t$  and number of lines parallel  $N$  of the samples. Curie temperature  $T_C$  and carrier concentration  $p$  were taken on reference samples from the corresponding wafers. Annealed samples are marked by "A".

to the diffusion constant. Using the Einstein relation  $\sigma = N(E_F)De^2$ , with the conductivity  $\sigma$ , the effective density of states at Fermi's energy,  $N(E_F)$ , can be determined.

To investigate electron-electron interaction in quasi 1D, 2D and 3D systems we fabricated Hall-bar mesas (2D and 3D) and wire arrays (1D and crossover regime from 1D to 2D) out of several wafers, having a  $(\text{Ga}_{1-x}\text{Mn}_x)$ As layer on top of semi-insulating GaAs. The nominal Mn-concentration  $x$  was approx. 4 % (sample  $1_{3D}$  and  $2_{3D}$ ) and  $\sim 6$  % (other samples). The relevant parameters of the samples are listed in table I. The dimensionality for EEI is defined by the number of spatial dimensions larger than the thermal diffusion length  $L_T = \sqrt{\hbar D/k_B T}$ . In (Ga,Mn)As  $L_T \approx 120 - 200$  nm at 20 mK, depending on the exact value of the diffusion constant  $D$ . Hence the thick Hall-bar mesas (150 nm and 300 nm) can be considered as quasi 3D, while the thin Hall-bar mesa (42 nm) is quasi 2D, at least below  $\sim 500$  mK. The smallest wires (42 nm and 35 nm) behave quasi 1D and the wider wires (62nm to 242 nm) are in the crossover regime from 1D to 2D, as is shown below. Arrays of wires with  $N$  wires in parallel were fabricated to suppress universal conductance fluctuations by ensemble averaging. The

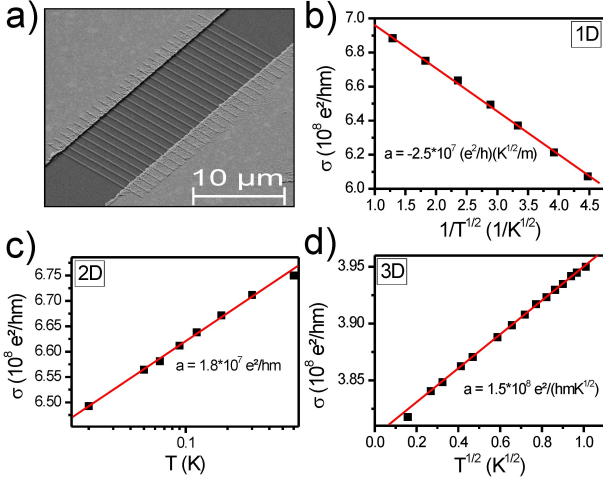


FIG. 1: a) Electron micrograph of a line array having 25 lines in parallel (Sample  $2_{1D-2D}A$ ). The width of the lines is 92 nm, the length is 10  $\mu\text{m}$ . b), c) and d): Conductivity of the quasi 1D line-array  $1_{1D}$  (b), the quasi 2D Hall-bar  $1_{2D}$  (c) and the quasi 3D Hall-bar  $2_{3D}$  (d) plotted versus temperature. The straight lines are guide for the eyes. The slope of the lines are given.

Hall-bars were fabricated using optical lithography and wet chemical etching. For fabricating the wire arrays we used electron-beam lithography and chemical dry etching. The contact pads to the devices were made by thermal evaporation of Au and lift-off. The measurements of the conductivity were performed in a top-loading dilution refrigerator using standard four-probe lock-in technique. To avoid heating of the charge carriers small measuring currents (25 pA to 4 nA, depending on the sample's resistance) and proper shielding were crucial. For each sample the measuring current was kept fixed for all temperatures. To suppress conductivity contributions due to weak localization we applied a perpendicular magnetic field of  $B = 3$  T. At  $B = 3$  T no weak localization can be observed in (Ga,Mn)As [13, 14] even at 20 mK.

According to Lee and Ramakrishnan [12] the temperature dependency of the conductivity correction due to EEI is depending on the dimensionality of the sample with respect to  $L_T$ . For 1D-systems the expected temperature dependency is  $\propto -1/\sqrt{T}$ , for 2D  $\propto \log_{10}(T/T_0)$  and for 3D  $\propto \sqrt{T}$ . Corresponding data for 1D, 2D and 3D (Ga,Mn)As-samples, shown in figure 1b-d), confirm the expected temperature dependency below 1 K. Hence the decreasing conductance with decreasing temperature in (Ga,Mn)As can be attributed to EEI.

The size of the conductivity correction due to electron-electron interaction is depending on the diffusion constant  $D$  in 1D-systems [12]:

$$\Delta\sigma = -\frac{F^{1D}}{\pi\omega t} \frac{e^2}{\hbar} \sqrt{\frac{\hbar D}{k_B T}}, \quad (1)$$

and also in 3D-systems [12]:

$$\Delta\sigma = \frac{F^{3D}}{4\pi^2} \frac{e^2}{\hbar} \sqrt{\frac{k_B T}{\hbar D}}. \quad (2)$$

As the conductivity correction due to EEI is also depending on the screening parameters  $F^{1D,2D,3D}$  one needs to know the corresponding parameter to extract  $D$  from the conductivity correction. Only in quasi 2D-systems the conductivity correction is independent on the diffusion constant [12]:

$$\Delta\sigma = \frac{F^{2D}}{2t\pi^2} \frac{e^2}{\hbar} \log \frac{T}{T_0}. \quad (3)$$

Hence in the 2D case  $F^{2D}$  can be directly extracted from experiment. As already shown in previous work [11] the screening parameter  $F^{2D}$  in (Ga,Mn)As ranges from 1.8 to 2.6 and is in excellent agreement with the screening parameter in Co, Co/Pt-multilayers and Permalloy. In these ferromagnetic metals  $F^{2D}$  is between 2.0 and 2.6 [15, 16, 17, 18]. Thus using the well known parameters  $F^{1D}$  of other ferromagnetic metals is a good approximation for  $F^{1D}$  in (Ga,Mn)As. In Ni and Py nanowires  $F^{1D}$  is 0.83 and 0.77 respectively [18, 19]. Consequently  $F^{1D} = 0.80 \pm 12$  should be a good approximation for the screening parameter of quasi 1D (Ga,Mn)As samples. With this  $F^{1D}$  parameter we can calculate the diffusion constant of sample  $1_{1D}$  using equation (1):  $D = 10 \pm 3 \cdot 10^{-5}$  m<sup>2</sup>/s. Using the Einstein relation this value corresponds to an effective density of states  $N(E_F) = 1.1 \pm 0.3 \cdot 10^{46}$  /Jm<sup>3</sup> at the Fermi energy. In figure 3  $N(E_F)$  is plotted versus the carrier concentration (green squares) for all investigated 1D-samples. Here, the uncertainty in determining the carrier concentration is  $\sim 10$  %.

It is more difficult to estimate the value of  $F^{3D}$  as no data are available for 3D ferromagnetic metals. Therefore we have to rely on theoretical predictions for the screening parameter:  $F^{3D} = 1.2$  [20]. Though the calculations of the 2D screening parameter ( $F^{2D} = 2.3$  [20]) agree well with the experimental values of different ferromagnets ( $F^{2D} = 1.8\dots 2.6$ ), they are less accurate for 1D systems. For 1D systems  $F^{1D}$  was calculated to be 1.6, while the typical experimental values of  $F^{1D} \approx 0.8$  are by a factor of 2 smaller [18, 19].

Hence by using the theoretical value for  $F^{3D}$  we need to take into account an uncertainty of order 100 %. Using equation (2) and the theoretical value for  $F^{3D} = 1.2$  [20] we arrive at  $D = 2.2 \cdot 10^{-5}$  m<sup>2</sup>/s for sample  $2_{3D}$ . Using the Einstein relation this corresponds to  $N(E_F) = 2.0 \cdot 10^{46}$  /Jm<sup>3</sup>, with a high uncertainty of approx. 200 %, as  $D$  is depending quadratically on  $F^{3D}$ .

The different temperature dependence of EEI in 1D ( $\Delta\sigma \propto -1/\sqrt{T}$ ) and 2D ( $\Delta\sigma \propto \ln T$ ) together with the temperature dependence of the thermal length  $L_T = \sqrt{\hbar D/k_B T}$  allows to use another scheme to extract the

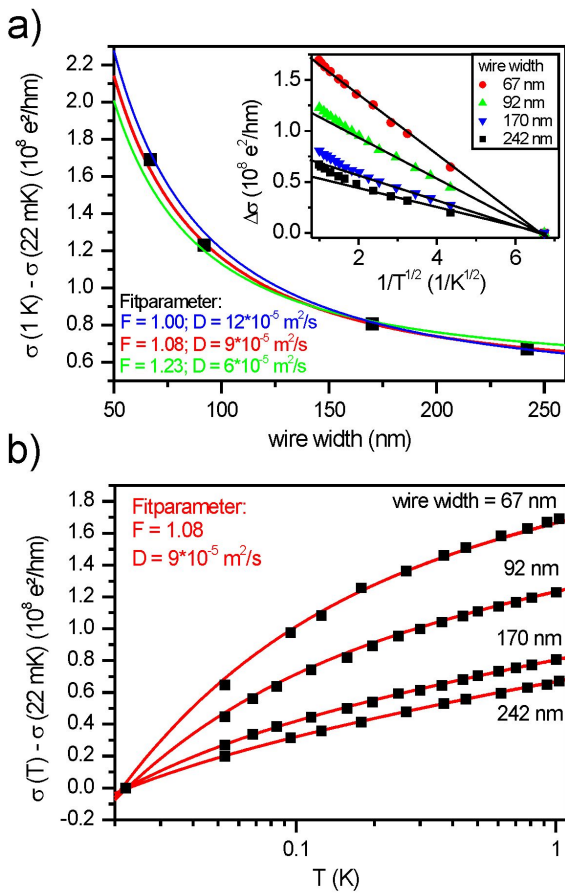


FIG. 2: a) Conductivity change from 1 K to 22 mK of four line arrays (sample  $1_{1D-2DA} \dots 4_{1D-2DA}$ ) plotted versus the wire width. The red line is the best fit of the data to equation (4). The blue and green lines are fits using equation (4) and a diffusion constant of  $12 \cdot 10^{-5} \text{ m}^2/\text{s}$  and  $6 \cdot 10^{-5} \text{ m}^2/\text{s}$  respectively. In the inset the conductivity change of four wire arrays (sample  $1_{1D-2DA} \dots 4_{1D-2DA}$ ) is plotted versus  $1/\sqrt{T}$ . The slopes are guide for the eyes. b) Conductivity change of the four line arrays (sample  $1_{1D-2DA} \dots 4_{1D-2DA}$ ) plotted versus temperature. The red lines are calculated using equation (4) and the parameters obtained by fitting the data in a).

diffusion constant and hence  $N(E_F)$ . By measuring the dimensional crossover, i.e. the change of the temperature dependence of the conductivity correction as a function of the sample size one can fit both, diffusion constant and screening parameter independently. Here we used the crossover from 1D to 2D to determine  $D$ . For this experiment wire arrays with wire widths, ranging from 62 nm to 242 nm (sample  $1_{1D-2DA} \dots 4_{1D-2DA}$  in table 1), were patterned on the same wafer. These four wires are in the crossover regime between 1D and 2D. This is most clearly seen in the inset of figure 2a and in figure 2b. In Fig. 2b the logarithmical temperature dependency, expected for 2D EEI, is only describing the widest wire at

high temperatures satisfactorily, while the  $1/\sqrt{T}$  dependency, expected for 1D EEI, only holds for the smallest wire at low temperatures in the inset of Fig. 2a. In the crossover regime the conductivity correction due to EEI is given by an interpolation formula [21]:

$$\Delta\sigma t = -F \frac{e^2}{\pi\hbar} \sum_{n=0}^{\infty} \left[ \frac{w^2}{L_T^2} + (n\pi)^2 \right]^{-1/2} - \left[ \frac{w^2}{L_{T_0}^2} + (n\pi)^2 \right]^{-1/2}, \quad (4)$$

with one screening parameter  $F$  and  $T_0$ , the lowest temperature. Figure 2a shows the conductivity change from 1 K to 22 mK of all four wire arrays. The conductivity change increases markedly with decreasing wire width. To extract the characteristic parameters we fitted the data using equation (4) with  $D$  and  $F$  as free parameters. The diffusion constant affects essentially the width dependence (x-scale) while the screening parameter  $F$  shifts the curve on the y-scale. Hence the fit is unique and allows to extract  $D$  and  $F$  independently. The best fitting result was obtained by using  $D = 9 \cdot 10^{-5} \text{ m}^2/\text{s}$  and  $F = 1.08$  (red line). To illustrate the sensitivity of the fitting procedure on  $D$  we also plotted equation (4) using  $D = 12 \cdot 10^{-5} \text{ m}^2/\text{s}$  (blue line) and  $D = 6 \cdot 10^{-5} \text{ m}^2/\text{s}$  (green line). Here  $F$  was the free parameter to optimize the fit. Both traces (blue and green) describe the experimental data less satisfyingly than the red trace. Hence the measurement of the dimensional crossover from 1D to 2D results in  $D = 9 \pm 1.5 \cdot 10^{-5} \text{ m}^2/\text{s}$ . In figure 2b the conductivity change with respect to 22 mK is plotted for all four wire arrays (sample  $1_{1D-2DA}$  to  $4_{1D-2DA}$ ) versus temperature. The red lines are the calculated conductivity correction given by equation (4). The parameters used were  $D = 9 \cdot 10^{-5} \text{ m}^2/\text{s}$  and  $F = 1.08$ . The conductivity correction in the whole temperature range from 22 mK to 1 K of all four wire arrays is perfectly described by using only these two parameters  $D$  and  $F$ . Also in the crossover regime from 1D to 2D the observed screening parameter  $F = 1.08$  is in excellent agreement with the screening parameter observed in Co ( $F = 0.95$ ) [15]. This underlines the universal character of the conductivity correction due to EEI. From the obtained diffusion constant we can estimate the effective density of states using the Einstein relation:  $N(E_F) = 1.6 \pm 0.3 \cdot 10^{46} / \text{Jm}^3$ .

To check the consistency of both presented methods, we can also treat the four samples ( $1_{1D-2DA}$  to  $4_{1D-2DA}$ ) as quasi 1D at low temperatures (indicated by the straight lines in the inset of figure 3a) and calculate the diffusion constant using equation (1) and  $F^{1D} = 0.8$  as described above. When doing so we obtain  $D = 8.4 \pm 2.5 \cdot 10^{-5} \text{ m}^2/\text{s}$ . This is in good agreement with the value estimated by fitting the crossover from 1D to 2D and hence the two methods are consistent.

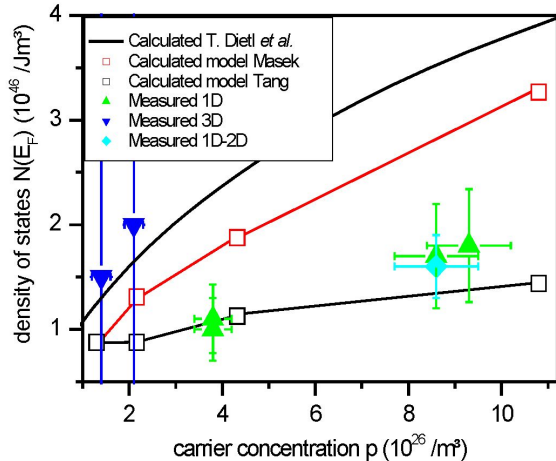


FIG. 3: Density of states at Fermi's energy plotted versus carrier concentrations. The squares are calculated using the model of Masek *et al.* and the model of Tang and Flattè respectively. The solid line gives  $N(E_F)$  calculated using a  $6 \times 6$   $k \cdot p$  model with parameters for the GaAs valence band [25]. The filled symbols are measured using EEI in 1D (green triangle), 3D (blue triangle) and in the crossover regime from 1D to 2D (blue diamond).

Figure 3 summarizes our findings and shows the extracted effective density of states versus the carrier concentration (filled symbols). The data are compared to calculations based on three different models: The solid line stems from a  $6 \times 6$   $k \cdot p$  model with parameters for the GaAs valence band, calculated by T. Dietl *et al.* and based on reference [25]. The corresponding effective hole mass is  $\sim 1m_e$  in the investigated range of carrier concentration. In addition we performed numerical simulations which are based on a multi-band tight-binding approach applied to disordered bulk systems using two different parameter sets. The first model was derived from first principles calculations for (Ga,Mn)As [22] (model Masek). The second one describes the Mn impurities by a modified on-site potential and a spin-dependent potential at the four nearest neighbor As sites which reproduce the experimental binding energy of 113 meV [23] (model Tang). A detailed description of the method and the two models is given in reference [24]. Neither model exhibits a detached impurity band for Mn concentrations larger than 1%. The effective masses were estimated to lie in the range  $m^* = 0.4...0.6m_e$  for the considered carrier concentrations with only minor quantitative differences between the two models. Due to the increasing number of holes the Fermi energy moves deeper into the valence band with increasing disorder. The experimental data for the density of states lie between the predicted values of the models. Although the data seem to be closer to the

model of Tang and Flattè, the relative high uncertainty of the experimental results does not allow to give a definite answer which model describes the experimental results better. For the case that Fermi's energy lies within a detached impurity band no calculations for the density of states are available. However assuming a parabolic band, one finds that  $N(E_F) \propto m^*$ , for a given carrier concentration. Hence an effective mass  $m^* \gg m_e$ , as expected for a detached impurity band, leads to an effective density of states at Fermi's energy far away from the measured values.

In conclusion we have demonstrated that the effective density of states at the Fermi energy of (Ga,Mn)As can be extracted from conductivity measurements, i.e. an analysis of the conductivity correction due to EEI. The measured values of  $N(E_F)$  are consistent with a picture that the Fermi energy is located within the GaAs valence band or an impurity band, merged with the valence band. Our experimental finding with effective masses of  $\sim 1m_e$  is however at odds with a detached impurity band, where the effective hole mass is much larger than  $m_e$ .

Acknowledgement: We thank T. Dietl and J. Fabian for stimulating discussions and the Deutsche Forschungsgemeinschaft (DFG) for their financial support via SFB 689.

\* Electronic address: daniel.neumaier@physik.uni-regensburg.de

† Present address: Fraunhofer ISE, Halle, Germany

‡ Present address: Institut für Angewandte Physik, University of Hamburg, Germany

- [1] H. Ohno, *Science* **281**, 951 (1998).
- [2] I. Žutić, J. Fabian, and S. Das Sarma, *Rev. Mod. Phys.* **76**, 323 (2004).
- [3] J. Fabian *et al.*, *Acta Phys. Slov.* **57**, 565 (2007).
- [4] K. Olejnik *et al.*, *Phys. Rev. B* **78**, 054403 (2008).
- [5] M. Wang *et al.*, arXiv:0808.1464v1 (unpublished).
- [6] T. Dietl *et al.*, *Science* **287**, 1019 (2000).
- [7] T. Jungwirth *et al.*, *Phys. Rev. B* **76**, 125206 (2007).
- [8] M. Sawicki, *J. Magn. Magn. Mater.* **300**, 1 (2006) and references therein.
- [9] K. S. Burch *et al.*, *Phys. Rev. Lett.* **97**, 087208 (2006).
- [10] K. Ando *et al.*, *Phys. Rev. Lett.* **100**, 067204 (2008).
- [11] D. Neumaier *et al.*, *Phys. Rev. B* **77**, 041306(R) (2008).
- [12] P. A. Lee and T. V. Ramakrishnan, *Rev. Mod. Phys.* **57**, 287 (1985).
- [13] D. Neumaier *et al.*, *Phys. Rev. Lett.* **99**, 116803 (2007).
- [14] L. P. Rokhinson *et al.*, *Phys. Rev. B* **76**, 161201(R) (2007).
- [15] M. Brands *et al.*, *Phys. Rev. B* **72**, 085457 (2005).
- [16] M. Brands *et al.*, *Phys. Rev. B* **74**, 033406 (2006).
- [17] M. Brands, A. Carl, and G. Dumpich, *Ann. Phys. (Leipzig)* **14**, 745 (2005).
- [18] D. Neumaier *et al.*, *Phys. Rev. B* **78**, 174424 (2008).
- [19] T. Ono *et al.*, *J. Magn. Magn. Mater.* **226**, 1831 (2001).
- [20] R. Raimondi, P. Schwab and C. Castellani, *Phys. Rev.* **60**, 5818 (1999).

- [21] G. Neuttiens *et al.*, Europhys. Lett. **34**, 617 (1996).
- [22] J. Masek *et al.*, Phys. Rev. B **75**, 045202 (2007).
- [23] J.-M. Tang and M. E. Flattè, Phys. Rev. Lett **92**, 047201 (2004).
- [24] M. Turek, J. Siewert, and J. Fabian, Phys. Rev. B **78**, 085211 (2008).
- [25] T. Dietl, H. Ohno, and F. Matsukura, Phys. Rev. B **63**, 195205 (2001).